

# Journal of Materials Chemistry A

Accepted Manuscript



This is an *Accepted Manuscript*, which has been through the Royal Society of Chemistry peer review process and has been accepted for publication.

*Accepted Manuscripts* are published online shortly after acceptance, before technical editing, formatting and proof reading. Using this free service, authors can make their results available to the community, in citable form, before we publish the edited article. We will replace this *Accepted Manuscript* with the edited and formatted *Advance Article* as soon as it is available.

You can find more information about *Accepted Manuscripts* in the [Information for Authors](#).

Please note that technical editing may introduce minor changes to the text and/or graphics, which may alter content. The journal's standard [Terms & Conditions](#) and the [Ethical guidelines](#) still apply. In no event shall the Royal Society of Chemistry be held responsible for any errors or omissions in this *Accepted Manuscript* or any consequences arising from the use of any information it contains.

# Hybrid Physical-Chemical Deposition Process at Ultra Low Temperatures for High-Performance Perovskite Solar Cells

Yanke Peng<sup>a†</sup>, Gaoshan Jing<sup>a†</sup> and Tianhong Cui<sup>\*ab</sup>

Quality of a perovskite film will directly determine the performance and stability of the corresponding perovskite solar cell. High-quality and uniform  $\text{CH}_3\text{NH}_3\text{PbI}_3$  films were synthesized by a new hybrid physical-chemical vapor deposition (HPCVD) process in a vacuum and isothermal environment. Reaction temperature can be accurately adjusted from 73 °C to 100 °C, with 73 °C as the lowest reaction temperature for a vapor based approach.  $\text{CH}_3\text{NH}_3\text{PbI}_3$  solar cells with high performance were fabricated at 82 °C to achieve high power conversion efficiency (PCE) up to 14.7%. The unsealed champion solar cell was tested for 31 days continuously, and its efficiency could maintain 12.1%, demonstrating high effectiveness of this HPCVD process.

## Introduction

Power conversion efficiency (PCE) record of the hybrid inorganic-organic perovskite solar cell developed at research labs has soared from 3.8% to 20.1% in five years (2009~2014),<sup>1,2</sup> comparable to the PCEs of GaAs thin film and silicon based solar cells constructed with nanostructures to increase light collection efficiency through light trapping or concentration.<sup>3-5</sup> The next great challenge that global researchers are facing is to develop high-performance and stable perovskite solar cells in cost efficient ways, so that this technology can compete with commercially available thin film photovoltaic technologies for probable broad applications, e.g. CdTe based solar cells, which has the lowest production cost among all solar cells currently.<sup>6</sup>

Performance of a perovskite solar cell is highly determined by the crystalline quality of the perovskite thin film sandwiched between electron and hole transport layers in a typical perovskite solar cell structure, such as the size of perovskite grains and the uniformity of the thin films.<sup>7-10</sup> There are two major type of methods to synthesize perovskite film, solution based (“wet”) and vapor based (“dry”) method. One key procedure to obtain high quality perovskite films is to optimize perovskite material reaction and crystallization rate. For two-step solution-based method, high quality perovskite film is rarely obtained due to high reaction rate between the solid  $\text{PbI}_2$  precursor film and the high concentration  $\text{CH}_3\text{NH}_3\text{I}/2$ -propanol (IPA) solution.<sup>11</sup> To reduce the perovskite reaction rate, a two-step spin-coating procedure was introduced by spin coating  $\text{CH}_3\text{NH}_3\text{I}/\text{IPA}$  solution with an optimized concentration on  $\text{PbI}_2$  precursor thin films.<sup>12</sup> For one step solution based method, additional chlorine based materials and procedures during spin coating are introduced to optimize the perovskite crystallization rate: (1) adding  $\text{PbCl}_2$ <sup>13</sup> or  $\text{CH}_3\text{NH}_3\text{Cl}$ <sup>14</sup> into a perovskite

solution for one-step spin coating; (2) dripping toluene when spin coating perovskite solution<sup>8</sup>, and (3) adding argon flow during solution spin-coating process to improve perovskite film quality.<sup>15</sup> Water vapor and oxygen in an ambient environment degenerate perovskite films so drastically that a nitrogen filled glove box was widely used to synthesize perovskite material for solution based methods.<sup>16, 17</sup> Nevertheless, it is still quite challenging to obtain high-quality, stable perovskite films using solution-based methods.

Perovskite thin films are synthesized by two solid precursors with large different material properties. One is lead halide, an inorganic material with an appropriate evaporation temperature about 320 °C, and the other is alkyl amino halide, an organic material with an appropriate temperature below 120 °C. Without proper gas precursors, conventional CVD system is not suitable for synthesizing perovskite films without modifying system configuration and deposition procedures. A few vapor based methods using modified PVD or CVD systems were developed to synthesize high-quality perovskite films, including dual-source vapor deposition,<sup>18, 19</sup> vapor assistant solution process (VASP),<sup>9, 20</sup> and hybrid chemical vapor deposition.<sup>21-24</sup> By dual-source vapor deposition method, a high-performance solar cell with 15.4% efficiency was fabricated when alkyl amino halide and lead halide were evaporated simultaneously in an high vacuum chamber, then deposited and reacted on a compact  $\text{TiO}_2/\text{FTO}$  substrate.<sup>18</sup> With VASP method, uniform  $\text{CH}_3\text{NH}_3\text{PbI}_3$  films with grain sizes as large as 500 nm and surface roughness as small as RMS 23.2 nm were synthesized in a glove box by reacting alkyl amino halide (e.g.,  $\text{CH}_3\text{NH}_3\text{I}$ ) vapor with solid  $\text{PbI}_2$  thin films. Corresponding perovskite solar cells exhibited high performance of 12.1% efficiency. Using a low pressure (0.3 Torr) VASP method,  $\text{PbI}_2/\text{PbCl}_2$  mixed halide precursors films

were annealed in  $\text{CH}_3\text{NH}_3\text{I}$  vapor at  $120^\circ\text{C}$  to synthesize perovskite films and the PCE of the best solar cell was up to 16.8% (reverse scanning) and 15.4% (forward scanning).<sup>20</sup> Another promising method is to use chemical vapor deposition method to synthesize perovskite films. High-quality perovskite nanoplatelets were grown on a muscovite mica surface by a hybrid CVD system with electron diffusion length over 200 nm.<sup>24</sup> A hybrid CVD method was dual temperature zones applied to synthesize perovskite films and form a solar cell with efficiency up to 11.8%.<sup>23</sup> In vapor based methods, the perovskite growth rate is determined by vapor reaction process, such as reaction temperature, vapor pressure, and vacuum level. Up to date, these vapor based methods cannot widely adapted because such parameters were difficult to adjust independently and accurately for high-quality perovskite material synthesis. Here, we introduce a new hybrid physical-chemical vapor deposition (HPCVD) method to synthesize high-quality perovskite films of  $\text{CH}_3\text{NH}_3\text{PbI}_3$ . Comparing to published vapor based methods,  $\text{CH}_3\text{NH}_3\text{PbI}_3$  thin films were synthesized in a well-controlled vacuum and isothermal environment. Critical reaction parameters, including vapor pressure and reaction temperature, can be adjusted accurately to further improve perovskite film quality. As shown in Figure 1,  $\text{PbI}_2$  solid thin film precursor (on mesoporous  $\text{TiO}_2$  (m- $\text{TiO}_2$ )/compact  $\text{TiO}_2$  (c- $\text{TiO}_2$ )/FTO substrates) and  $\text{CH}_3\text{NH}_3\text{I}$  crystal solid precursor were placed into a quartz boat and then put inside an isothermal vacuum quartz tube. By heating up to a certain temperature, the evaporated  $\text{CH}_3\text{NH}_3\text{I}$  vapor reacted with the solid  $\text{PbI}_2$  films to synthesize uniform  $\text{CH}_3\text{NH}_3\text{PbI}_3$  thin films. In this method, vacuum level of 2 mTorr is maintained to reduce perovskite film defects. Due to the easy sublimation of organic precursor  $\text{CH}_3\text{NH}_3\text{I}$  heated at  $70^\circ\text{C}$  or above, the pressure in the quartz tube was about 15~30 mTorr under vacuum pumping. With two quartz blocks at the ends of the quartz tube,  $\text{CH}_3\text{NH}_3\text{I}$  vapor pressure on the  $\text{PbI}_2$  film surface can be maintained in a “quasi” stable status during vacuum pumping. Meanwhile, the pressure can be changed by adjusting placement configuration between these two precursor materials. Constant reaction temperature between  $73^\circ\text{C}$ ~ $100^\circ\text{C}$  was set to synthesize high-quality  $\text{CH}_3\text{NH}_3\text{PbI}_3$  thin films, with  $73^\circ\text{C}$  as the lowest temperature to

cell was tested for 31 days continuously, and its reverse scan mode efficiency can still maintain 12.1%, demonstrating the effectiveness and stability of this new HPCVD method. This vacuum and vapor based method is compatible with conventional semiconductor fabrication methods, and high-quality perovskite films can be achieved through delicate process control. Eventually, perovskite based solar cells could be mass produced in low cost for large-scale applications by this new method.

## Experimental

### Synthesis of $\text{CH}_3\text{NH}_3\text{I}$

Methylamine (27.86 ml, 40% in methanol, Sigma) and hydroiodic acid (30 ml, 57 wt% in water, Aldrich) were mixed at  $0^\circ\text{C}$  and stirred for 2 h. The precipitate was recovered by evaporation at  $50^\circ\text{C}$  for 1 h. The product was washed with diethyl ether three times and finally dried at  $60^\circ\text{C}$  in a vacuum oven for 24 h.

### Substrate preparation

FTO-coated glass sheets ( $20\times 20$  mm, Tec15, Pilkington, St Helens, United Kingdom) were patterned by a laser cutter. These sheets were then cleaned by ultra-sonication in deionized (DI) water, ethanol, acetone, isopropyl alcohol (IPA) and DI water sequentially for 15 min, respectively. Finally, they were treated in an oxygen plasma asher (PDC-32G-2, Henniker Plasma, Warrington, UK) for 15 min to remove the organic residues on the surfaces.

### Solar cells fabrication

An acidic solution of titanium isopropoxide<sup>18</sup> (Sigma-Aldrich, 99.999%, St. Louis, USA) in ethanol was spin-coated onto the clean FTO sheet at 2000 rpm for 40 s, and then sintering at  $500^\circ\text{C}$  for 30 min to form a compact  $\text{TiO}_2$  layer with a thickness of 20~40 nm. The mesoporous  $\text{TiO}_2$  layer was deposited by spin coating at 5000 rpm for 15 s using a commercial  $\text{TiO}_2$  paste (NJU-SR, Sunlaite, Suzhou, China) diluted in ethanol (1:4, weight ratio). After baking at  $120^\circ\text{C}$  for 10 min, the mesoporous  $\text{TiO}_2$  films were sintered at  $500^\circ\text{C}$  for 30 min and then cooled to room temperature. The substrates were treated in a 50 mM aqueous solution of  $\text{TiCl}_4$  for 30 min at  $70^\circ\text{C}$ , rinsed with DI water and ethanol and dried at  $500^\circ\text{C}$  for 30 min.  $\text{PbI}_2$  was dissolved in N, N-dimethylformamide (DMF, Sigma, St. Louis, USA) at a concentration of  $461\text{ mg mL}^{-1}$  under stirring at  $70^\circ\text{C}$ . The solution was kept at  $70^\circ\text{C}$  during the whole procedure and  $\text{TiO}_2$  substrates were pre-heated at  $70^\circ\text{C}$ .  $80\ \mu\text{L}$  of  $\text{PbI}_2/\text{DMF}$  solution was spin-coated on each substrate at 4500 rpm for 20 s in ambient air with the relative humidity below 30%. After heated at  $70^\circ\text{C}$  in the air for 30 min, the  $\text{PbI}_2$  substrates were laid upon the  $\text{CH}_3\text{NH}_3\text{I}$  powder with  $\text{PbI}_2$  side back to the powder in a quartz boat. Then, the boated filled with  $\text{CH}_3\text{NH}_3\text{I}$  powder and  $\text{PbI}_2$  substrates were put into the quartz tube. After flanges were mounted on the tube, the vacuum in the tube was pumped to 10 mTorr. Then,

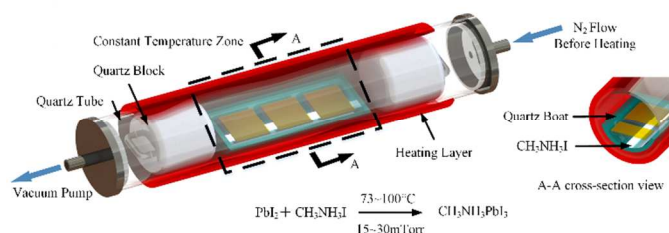


**Fig. 1** Schematic diagram of a hybrid physical-chemical vapor deposition (HPCVD) method for synthesizing perovskite ( $\text{CH}_3\text{NH}_3\text{PbI}_3$ ) films.

synthesize perovskite film so far as we know. Highly uniform perovskite films were synthesized, and high PCE up to 14.7% (reverse scanning) and 11.5% (forward scanning) at  $82^\circ\text{C}$  was achieved for these solar cells. The unsealed champion solar

50 sccm nitrogen flow was input into the tube to clean the inner surface for 20 min. When the valve of the nitrogen flow was shut down, the vacuum in the quartz tube could increase to 2 mTorr. 80, 90, 100, 110 °C were set as the heating temperature in the furnace control program, but the real temperature in the tube was 73, 82, 90, 100 °C respectively, which was calibrated by a wireless PT1000 temperature recorder (TP-1000-W1, A-Volt Co., Ltd, Beijing, China) laid in the vacuum quartz tube during the heating procedures. The actual temperature curve inner the quartz tube is shown in Figure S1. After three hours reaction in the quartz tube, the perovskite films were annealed at 100 °C for 10 min at relative humidity 30% ± 5% in ambient environment by following a published procedure for a high efficiency solar cell fabrication method.<sup>10, 25</sup> Then 150 nm Spiro-OMeTAD was spin-coated onto the perovskite films at 4000 rpm according to previous reported methods.<sup>12</sup> Finally, 60 nm gold electrode was then deposited by E-beam evaporation. Active area of a typical solar cell was 0.16 cm<sup>2</sup>.

### Characterization

A field-emission scanning electron microscope (FE-SEM, Zeiss Merlin) was used to investigate the surface and cross-sectional morphology of the perovskite solar cells. Current density-voltage (*J-V*) curves were measured using an Agilent B1500A Semiconductor Device Parameter Analyser, which can measure the current-voltage curve of samples at pA level. The measurements were carried out under AM1.5G illumination at 100 mW/cm<sup>2</sup> provided by a Newport ABB (94021A) solar simulator in ambient air. Light intensity was calibrated with a

Newport calibrated mono-Si reference cell (Newport calibration cert. #0702). A testing mask was used during the measurements with active area of 0.09 cm<sup>2</sup>. The *J-V* curves were obtained in the air (1.2 V ~ -0.1 V ~ 1.2 V) with the step size of 20 mV. Delay time at every measurement point is 50 ms. Incident Photon to Current Conversion Efficiencies (IPCE) were measured using an Oriel IQE 200 equipment.

### Results and discussion

In HPCVD method, two critical parameters, CH<sub>3</sub>NH<sub>3</sub>I vapor pressure and reaction temperature, can be delicately adjusted to synthesize high-quality CH<sub>3</sub>NH<sub>3</sub>PbI<sub>3</sub> films. As shown in Figure 1, a vacuum pump was kept running and the CH<sub>3</sub>NH<sub>3</sub>I was kept sublimating during the process to prevent from leakage contamination through an ambient environment, so that the pressure inside the quartz tube is not a same value. There would exist the highest pressure around the quartz boat containing CH<sub>3</sub>NH<sub>3</sub>I precursor crystal, which is close to the CH<sub>3</sub>NH<sub>3</sub>I vapor pressure at specific reaction temperature. Meantime, there would have the lowest pressure at the end of the quartz tube (equal to 2 mTorr). Because of the existence of two quartz blocks, pressure gradient profile inside the tube should be maintained in a stable status without vapor convection turbulence. To demonstrate this hypothesis, we arranged two precursor materials in two placement configuration shown in Figure 2(a) and (b): one is “face to face”; another is “back to

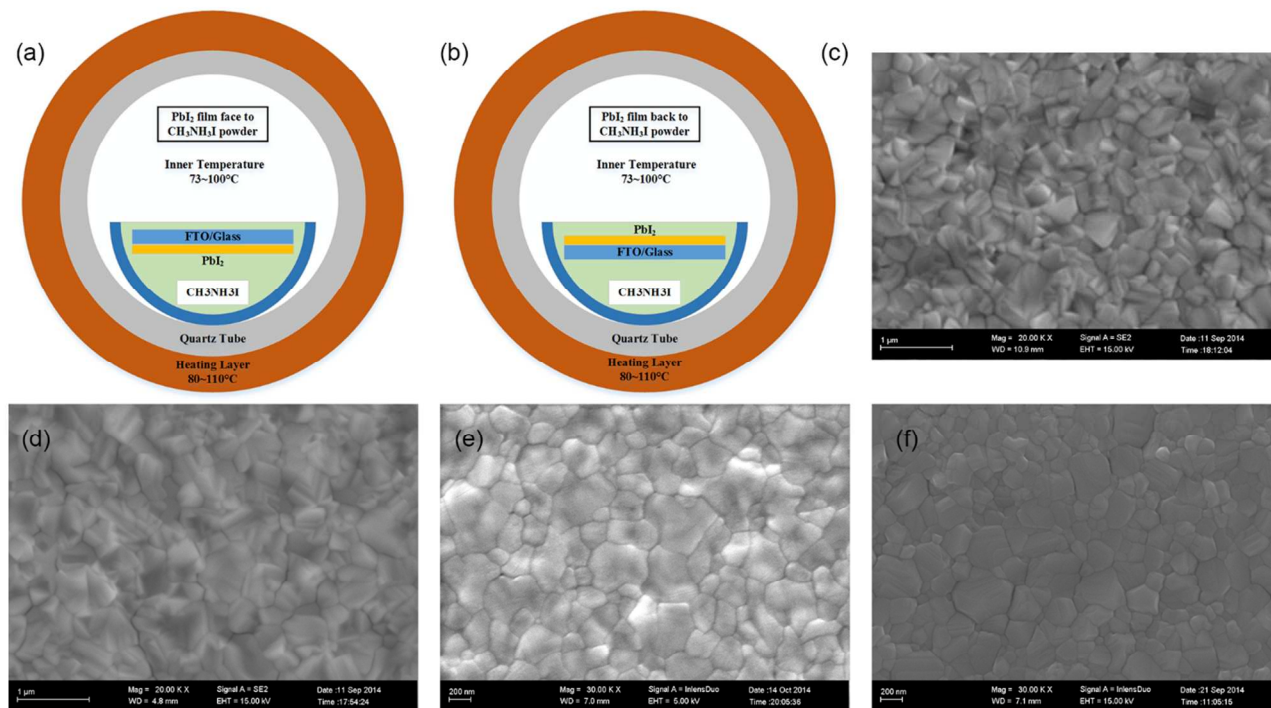


Figure 2. Schematic diagrams of two precursor material (PbI<sub>2</sub> thin film and CH<sub>3</sub>NH<sub>3</sub>I powder crystal) placement configurations in HPCVD process: (a) “face to face” configuration (b) “back to face” configuration. Top view scanning electron microscopy (SEM) images of CH<sub>3</sub>NH<sub>3</sub>PbI<sub>3</sub> films formed by HPCVD at 100 °C: (c) “face to face” configuration before annealing; (d) “face to face” configuration after annealing at 100 °C for 10 min; (e) “back to face” configuration before annealing; (f) “back to face” configuration after annealing at 100 °C for 10 min in ambient air under relative humidity of (RH) 30% ± 5%.

face".  $\text{CH}_3\text{NH}_3\text{I}$  vapor pressure on the  $\text{PbI}_2$  surface in "face to face" configuration should larger than that of "back to face" due to the blockage by the FTO substrate. Therefore,  $\text{CH}_3\text{NH}_3\text{PbI}_3$  reaction in the "back to face" configuration should have slower reaction rate than that of "face to face". As shown in Fig. 2c and Fig. 2e, a typical  $\text{CH}_3\text{NH}_3\text{PbI}_3$  film synthesized in "back to face" configuration is more uniform than its counterpart in "face to face" configuration, probably because of lower reaction rate. Surface profile difference became more apparent after post thermal annealing process at 100 °C for 10 min in ambient air under relative humidity 30%  $\pm$  5%, as shown in Fig. 2d and Fig. 2f. To obtain a  $\text{CH}_3\text{NH}_3\text{PbI}_3$  film with better surface uniformity, we chose the "back to face" configuration in the HPCVD process. XRD spectra of the HPCVD perovskite films<sup>26</sup> shows strong peaks at 14.18°, 28.52°, 31.96°, corresponding to (110), (220), (310) miller indices of  $\text{CH}_3\text{NH}_3\text{PbI}_3$  perovskite crystal. Compared with the XRD spectra of traditional two-step solution method,<sup>11</sup> the relative heights and the full widths at half maximum (FWHM) of these peaks exhibit a better crystalline quality of HPCVD perovskite films. It should be noted that the emergence of a peak at 12.65° after post annealing process could be resulted from self-induced passivation of  $\text{PbI}_2$  on perovskite grain structure surfaces, which could improve performance of the solar cells.<sup>10, 25</sup> Besides  $\text{CH}_3\text{NH}_3\text{I}$  vapor pressure, reaction temperature (73 °C, 82 °C, 90 °C, and 100 °C) can be accurately

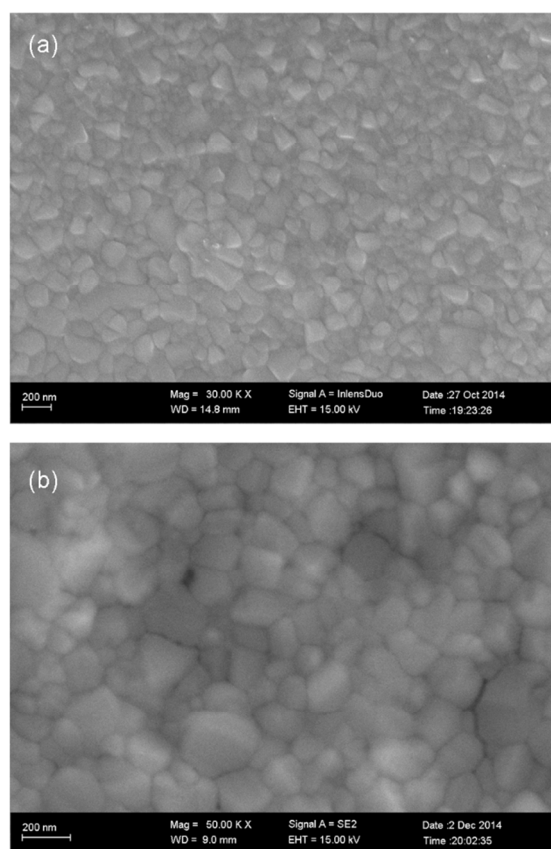
adjusted to synthesize perovskite films. Uniform  $\text{CH}_3\text{NH}_3\text{PbI}_3$  films can be obtained at 73 °C, which is the lowest reaction temperature for vapor based methods. Comparing two films shown in Fig. 2e and Fig. 3a, larger crystalline size and more uniform surface were likely to be achieved at high reaction temperatures.

**Table 1** PCE statistics of perovskite solar cells with  $\text{CH}_3\text{NH}_3\text{PbI}_3$  films synthesized at different reaction temperatures

Group	No. total	Mean	Standard Deviation	Min	Median	Max
100 °C	27	11.1%	2.07%	6.2%	11.5%	14.2%
90 °C	9	11.7%	1.96%	8.7%	12.5%	14.1%
82 °C	26	11.4%	2.10%	6.9%	11.3%	14.7%
73 °C	27	12.0%	1.12%	10.1%	12.3%	14.1%

Efficiencies statistics of solar cells obtained with  $\text{CH}_3\text{NH}_3\text{PbI}_3$  films constructed by the HPCVD method at 73 °C, 82 °C, 90 °C and 100 °C are shown in Fig. 4. Detailed information of these solar cells is reported in supplementary information. Though the solar cell with the best performance (champion cell, PCE: 14.7% (reverse scanning mode) and 11.5% (forward scanning mode)) was obtained at 82 °C, devices obtained at 73 °C has the smallest PCE standard deviation comparing to that of devices obtained at 82 °C, 90 °C and 100 °C shown in Table 1. The reason may be that the pressure gradient profile at 73 °C is smaller than that at 82 °C, 90 °C and 100 °C,  $\text{CH}_3\text{NH}_3\text{PbI}_3$  films were synthesized in a relative "quasi constant pressure" environment.

High performance  $\text{CH}_3\text{NH}_3\text{PbI}_3$  solar cells were obtained by HPCVD method at ultra-low temperature of 73 °C. An SEM cross-sectional image of the gold/Spiro-OMeTAD/ $\text{CH}_3\text{NH}_3\text{PbI}_3$ /m-TiO<sub>2</sub>/c-TiO<sub>2</sub>/FTO perovskite solar cell is shown in Fig. 5a. Uniform  $\text{CH}_3\text{NH}_3\text{PbI}_3$  film about 250 nm thick was sandwiched between the hole transport layer (Spiro-OMeTAD) and the electron transport layer (m-TiO<sub>2</sub>). As show in Fig. 5b, the best



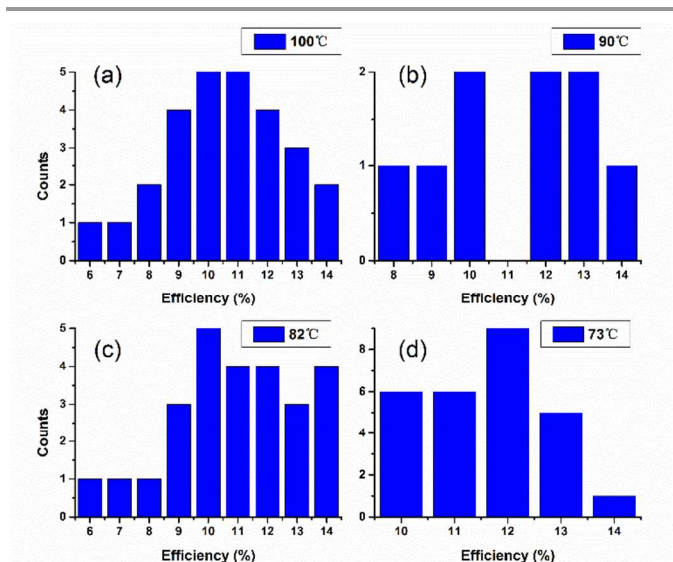


Figure 4. Power conversion efficiency (PCE) statistics of perovskite solar cells with  $\text{CH}_3\text{NH}_3\text{PbI}_3$  films synthesized at different reaction temperatures.

device by HPCVD at  $73^\circ\text{C}$  exhibits great performance, with reverse scan:  $J_{SC} = 22.63 \text{ mA/cm}^2$ ,  $V_{OC} = 1.05 \text{ V}$ , filling factor ( $FF$ ) = 60%, PCE = 14.1%; forward scan:  $J_{SC} = 22.81 \text{ mA/cm}^2$ ,  $V_{OC} = 1.02 \text{ V}$ , filling factor ( $FF$ ) = 49%, PCE = 11.2%. External quantum efficiency (EQE) spectrum is shown in Fig. 5c.

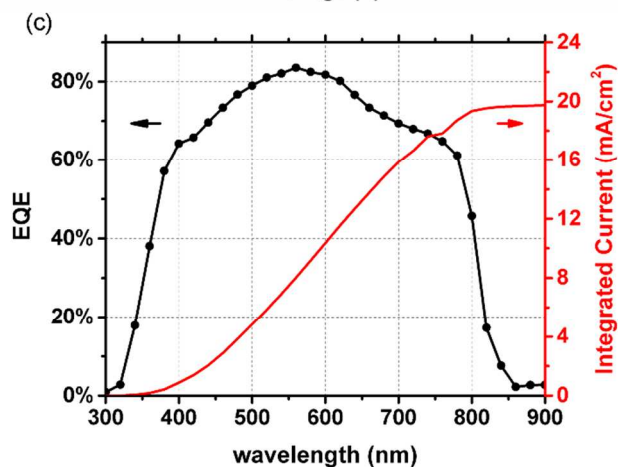
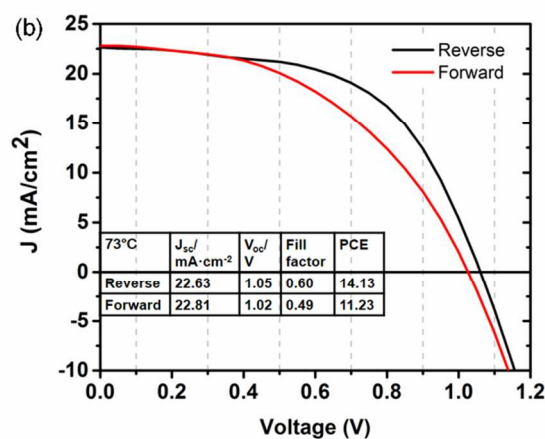
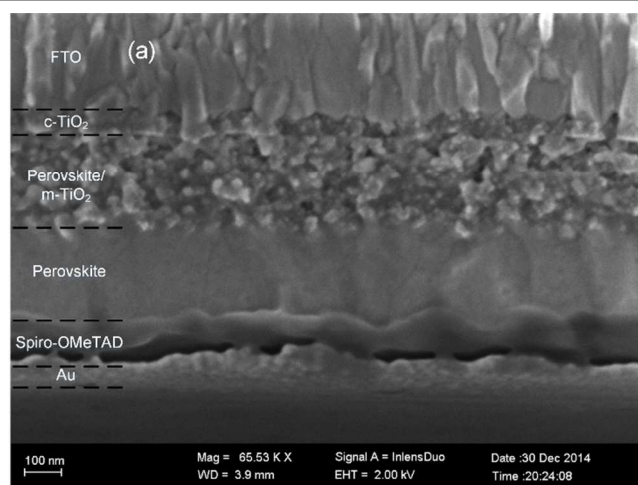


Fig. 5 (a) Cross-sectional view SEM image of a completed solar cell constructed from a HPCVD  $\text{CH}_3\text{NH}_3\text{PbI}_3$  film about 250 nm thick at  $73^\circ\text{C}$  for 150 min. (b) Current-density vs voltage curves of the best performing solar cell fabricated by the same process measured under simulated AM1.5 sunlight of  $100 \text{ mW/cm}^2$  irradiance. (c) External quantum efficiency (EQE) spectrum of this device with integrated current density of  $19.8 \text{ mA/cm}^2$ .

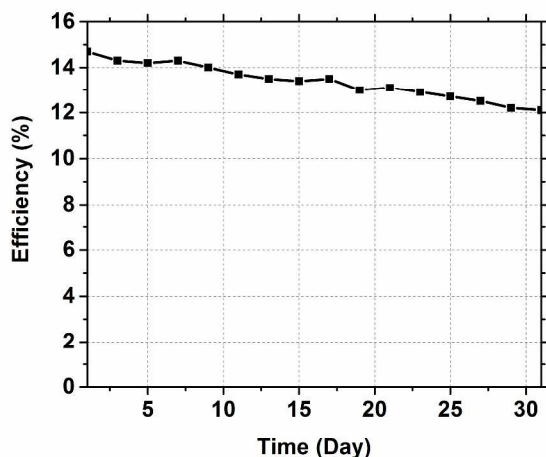


Figure 6. PCE decay curve of the champion perovskite solar cell (reverse scan mode: 14.7%). The unsealed champion cell was tested every day in ambient environment with relative humidity below 30% to characterize its long-term stability. After 31 days testing, its efficiency maintained 12.1% (reverse scan mode). The device was stored in a vessel with phosphorous oxide as the desiccant.

Integrating the overlap of the EQE spectrum with the AM 1.5G solar photon flux yields a current density of 19.8 mA/cm<sup>2</sup>, lower than  $J_{SC}$  from the  $J-V$  curve. It probably be attributed to the surface trap of the TiO<sub>2</sub> transport layer reported previously. Compared to existing vapor based methods<sup>9, 18-24</sup>, high performance perovskite solar cells by HPCVD were achieved under ultra-low temperature of 73 °C. Meanwhile, lead precursor cannot be fully converted into perovskite material at annealing temperature of 100 °C for LP-VASP<sup>20</sup> and perovskite film was synthesized at 150 °C using VSAP<sup>9</sup>. It could be the maintained high vacuum level (2 mTorr) prior to HPCVD process that leads to such a low synthesis temperature. Theoretically, these vapor based process can be divided into three sequential processes: (1) physical vapor deposition (PVD) process: CH<sub>3</sub>NH<sub>3</sub>I powder is evaporated and CH<sub>3</sub>NH<sub>3</sub>I vapor arrives onto a solid substrate with a perovskite film synthesized beforehand, with a PbI<sub>2</sub> precursor film underneath; (2) gas phase/solid phase transportation process: CH<sub>3</sub>NH<sub>3</sub>I vapor diffuses through the solid perovskite film and onto the PbI<sub>2</sub> precursor film surface; (3) surface reaction process: CH<sub>3</sub>NH<sub>3</sub>I vapor reacts with the PbI<sub>2</sub> precursor film, and thickness of the perovskite layer increases. For the PVD process determined by pressure and temperatures, evaporation rate of CH<sub>3</sub>NH<sub>3</sub>I vapor can be described by the following formula<sup>27</sup>:

$$\Gamma = 5.84 \times 10^{-2} \left(\frac{M}{T}\right)^{\frac{1}{2}} (P_e - P_h) \quad g/cm^2 \cdot s \quad (1)$$

where  $M$  is the molecular weight of CH<sub>3</sub>NH<sub>3</sub>I,  $T$  is the temperature,  $P_e$  is the vapor pressure of CH<sub>3</sub>NH<sub>3</sub>I at specific temperature and  $P_h$  is the chamber pressure.

At a certain temperature, vapor pressure of CH<sub>3</sub>NH<sub>3</sub>I ( $P_e$ ) is a constant under an equilibrium state. The higher the chamber pressure ( $P_h$ ), the lower evaporation rate can be achieved for

CH<sub>3</sub>NH<sub>3</sub>I vapor. Lower evaporation rate can lead to slower CH<sub>3</sub>NH<sub>3</sub>I vapor diffusion rate and smaller surface reaction rate. Eventually, when thickness of PbI<sub>2</sub> film is over a certain threshold, full conversion of the precursor film is not feasible. For VSAP, LP-VASP and HPCVD methods,  $P_h$  is 760 Torr<sup>9</sup>, 0.3 Torr<sup>20</sup> and 2 mTorr, respectively, which may explain perovskite films 200~300 nm thick should be synthesized at 150 °C by VSAP, 120 °C by LP-VASP, while 73 °C (even for “back to face” configuration with a slower growth rate) by HPCVD. In addition, the PbI<sub>2</sub> precursor film could not be fully converted into a perovskite film after twelve hours of reaction at 60 °C by HPCVD. Further investigations on HPCVD’s reaction kinetics is underway.

Finally, a long-term stability test was done for the champion cell obtained at 82 °C. The unsealed champion solar cell was tested for 31 days continuously, and its reverse scan mode efficiency can still maintain 81% of its initial efficiency (12.1% vs 14.7%), demonstrating the effectiveness and stability of this new HPCVD method, compared to the reported unsealed perovskite solar cell which decayed rapidly during storage period<sup>10</sup>. The relative high performance in long-term stability may contribute to the low vacuum level environment for synthesizing perovskite material. Inside the quartz tube, concentrations of corrosive molecules, such as water vapor, oxygen and organic chemicals, are much lower than that in an ambient environment or a glove box so that much less corrosive molecules are trapped inside the perovskite material. As the perovskite solar cells were tested or stored in atmosphere, water vapor and oxygen in ambient environment would **gradually diffuse** into the perovskite material so that the solar cell’s performance slowly degraded for a testing period of 31 days. However, due to very few corrosive molecules were trapped into the perovskite material synthesized in a high vacuum, performance decay rate of the perovskite solar cell by HPCVD was much slower than that of perovskite solar cells fabricated in an ambient air. Further investigation on perovskite film defects is underway.

## Conclusion

In summary, high-quality CH<sub>3</sub>NH<sub>3</sub>PbI<sub>3</sub> films and corresponding solar cells were prepared by a new hybrid physical-chemical vapor deposition (HPCVD). In this method, vapor pressure can be adjusted by changing the configuration of PbI<sub>2</sub> substrate. Reaction temperature can be accurately adjusted from 73 °C~100 °C. By optimizing these reaction parameters, high performance CH<sub>3</sub>NH<sub>3</sub>PbI<sub>3</sub> solar cells were fabricated to achieve high power conversion efficiency up to 14.7%. The unsealed champion solar cell was tested for continuous 31 days, and its efficiency (reverse scan mode) can still maintained 12.1%. High stability of such devices could be due to the highly uniform perovskite film synthesized in vacuum environment, free of water vapor/oxygen contamination. Slow reaction rate to synthesize dense material could further increase the stability of the devices. In future, parameters of this HPCVD method (vacuum level, reaction temperature, reaction time, etc.) could

be further optimized respectively to achieve solar devices with better performance. Eventually, perovskite solar cells could be mass produced in low cost for large-scale applications by this new method.

### Acknowledgements

This work was financially supported by the International Science and Technology Cooperation Program of Ministry of Science and Technology of the People's Republic of China (Grant No. 2013DFA51800).

### Notes and references

<sup>a</sup> State Key Laboratory of Precision Measurement Technology and Instruments, Department of Precision Instruments, Tsinghua University, Beijing, 100084, China

<sup>b</sup> Department of Mechanical Engineering, University of Minnesota, Minneapolis, Minnesota 55455, USA. Phone: 001-612-626-1636

Email: tcui@me.umn.edu

† The first two authors contributed equally to this work.

Electronic Supplementary Information (ESI) available: [Photovoltaic parameters of solar cells structured from CH<sub>3</sub>NH<sub>3</sub>PbI<sub>3</sub> film by HPCVD at 73, 82, 90, 100 °C].

1. A. Kojima, K. Teshima, Y. Shirai and T. Miyasaka, *Journal of the American Chemical Society*, 2009, **131**, 6050-6051.
2. [http://www.nrel.gov/ncpv/images/efficiency\\_chart.jpg](http://www.nrel.gov/ncpv/images/efficiency_chart.jpg), Accessed 02-04, 2015.
3. J. Yang, F. Luo, T. S. Kao, X. Li, G. W. Ho, J. Teng, X. Luo and M. Hong, *Light: Science & Applications*, 2014, **3**, e185.
4. M. Memarian and G. V. Eleftheriades, *Light: Science & Applications*, 2013, **2**, e114.
5. E. D. Kosten, J. H. Atwater, J. Parsons, A. Polman and H. A. Atwater, *Light: Science & Applications*, 2013, **2**, e45.
6. Advance PV modules, <http://www.firstsolar.com/en/technologies-and-capabilities/pv-modules>, Accessed Mar. 22, 2015.
7. C. Wehrenfennig, M. Liu, H. J. Snaith, M. B. Johnston and I. Herz, *Energy & Environmental Science*, 2014.
8. N. J. Jeon, J. H. Noh, Y. C. Kim, W. S. Yang, S. Ryu and S. I. Seok, *Nature materials*, 2014, **13**, 897-903.
9. Q. Chen, H. Zhou, Z. Hong, S. Luo, H. S. Duan, H. H. Wang, Y. Liu, G. Li and Y. Yang, *Journal of the American Chemical Society*, 2014, **136**, 622-625.
10. H. Zhou, Q. Chen, G. Li, S. Luo, T. b. Song, H. S. Duan, Z. Hong, J. You, Y. Liu and Y. Yang, *Science*, 2014, **345**, 542-546.
11. J. Burschka, N. Pellet, S. J. Moon, R. Humphry-Baker, P. Gao, M. K. Nazeeruddin and M. Gratzel, *Nature*, 2013, **499**, 316-319.
12. J. H. Im, I. H. Jang, N. Pellet, M. Gratzel and N. G. Park, *Nature nanotechnology*, 2014, **9**, 927-932.
13. M. M. Lee, J. Teuscher, T. Miyasaka, T. N. Murakami and H. J. Snaith, *Science*, 2012, **338**, 643-647.
14. Y. Zhao and K. Zhu, *The Journal of Physical Chemistry C*, 2014, 140416115637006.
15. F. Huang, Y. Dkhissi, W. Huang, M. Xiao, I. Benesperi, S. Rubanov, Y. Zhu, X. Lin, L. Jiang, Y. Zhou, A. Gray-Weale, J. Etheridge, C. R. McNeill, R. A. Caruso, U. Bach, L. Spiccia and Y.-B. Cheng, *Nano Energy*, 2014.
16. W. Li, H. Dong, L. Wang, N. Li, X. Guo, J. Li and Y. Qiu, *Journal of Materials Chemistry A*, 2014, **2**, 13587-13592.
17. G. Niu, X. Guo and L. Wang, *Journal of Materials Chemistry A*, 2015.
18. M. Liu, M. B. Johnston and H. J. Snaith, *Nature*, 2013, **501**, 395-398.
19. B.-S. Kim, T.-M. Kim, M.-S. Choi, H.-S. Shim and J.-J. Kim, *Organic Electronics*, 2015, **17**, 102-106.
20. Y. Li, J. K. Cooper, R. Buonsanti, C. Giannini, Y. Liu, F. M. Toma and I. D. Sharp, *The Journal of Physical Chemistry Letters*, 2015, **6**, 493-499.
21. D. J. Lewis and P. O'Brien, *Chemical communications*, 2014, **50**, 6319-6321.
22. P. Luo, Z. Liu, W. Xia, C. Yuan, J. Cheng and Y. Lu, *ACS applied materials & interfaces*, 2015.
23. M. R. Leyden, L. K. Ono, S. R. Raga, Y. Kato, S. Wang and Y. Qi, *J. Mater. Chem. A*, 2014.
24. S. T. Ha, X. F. Liu, Q. Zhang, D. Giovanni, T. C. Sum and Q. H. Xiong, *Advanced Optical Materials*, 2014, **2**, 838-844.
25. J. You, Y. M. Yang, Z. Hong, T.-B. Song, L. Meng, Y. Liu, C. Jiang, H. Zhou, W.-H. Chang and G. Li, *Applied Physics Letters*, 2014, **105**, 183902.
26. Y. Peng, G. Jing and T. Cui, in *MRS Spring 2015*, San Francisco, 2015.
27. O. Milton, *Materials Science of Thin Films*, Academic Press, San Diego, 2002.